Electron−Nucleus Resonances and Magnetic Field Accelerations in the Ortho−Para H_2 Conversion

S. Paris and E. Ilisca*

Laboratoire de Physique Théorique de la Matière Condensée, Université Paris, 7-Denis-Diderot, 7020, 2 place Jussieu, 75251 Paris Cedex 05, France

Received: January 5, 1999; In Final Form: March 1, 1999

The ortho−para conversion rate of hydrogen molecules physisorbed on transition metal oxides is shown to be drastically enhanced for selected values of the parameters. This new electron−nucleus resonant mechanism is suggested to interpret the observed accelerations of the conversion rate by an external magnetic field. The sensitivity of the magnetic field acceleration upon catalyst pretreatments might have important practical applications in the selection and preparation of industrial catalysts.

I. Introduction

The existence of the two nuclear spin isomers of molecular hydrogen, denoted ortho and para, was associated with the presence of nuclear spins in the early development of quantum mechanics. The ortho (respectively, para) variety is characterized by a triplet (respectively, singlet) nuclear spin state and by odd (respectively, even) rotational states.[1] The conversion process from one isomer to another entails the presence of a catalyst. It occurs during the scattering of the hydrogen molecules on the catalyst magnetic impurities. These create strong magnetic field gradients able to uncouple the hydrogen proton spins.[2] This process has important industrial applications, particularly in aerospace, since the conversion is a necessary step in the liquefaction and storage of molecular hydrogen.[3]

It was recognized in the 60's that transition metal oxides provide efficient catalysts.[4] These were built in dispersing 3d magnetic ions at the surface of a diamagnetic substrate. A typical system extensively investigated consists of different concentrations of chromia impurities inserted in an alumina substrate. While performing ortho−para (o−p) conversion experiments on such catalysts, Misono and Selwood (M.S.)[5,6] discovered in 1968 the sensitivity of the conversion rates upon the application of an external and homogeneous magnetic field H. The conversion was accelerated and the rate found to be growing linearly with H at low field ($H < 1$ kG) and saturating at moderately high field ($H > 5$ kG). At saturation, the field acceleration could reach 75% for magnetically diluted chromia catalysts. In 1976, similar results were obtained on cobalt and manganese oxides.[7] On CoO, the acceleration was found to be slightly negative at low field ($H < 4$ kG) and then grew without reaching saturation up to 20% at $H = 20$ kG. On MnO, the acceleration was positive and much faster (200% at $H = 20$ kG and not completely saturated). Different patterns were also obtained on rare-earth catalysts,[8] but in this paper we shall restrict ourselves to 3d ions.

These observations appeared very surprising and have never been understood. First, a homogeneous magnetic field induces a simultaneous precession of the nuclear spins, whereas the ortho−para transition needs their dephasing. Second, the magnetic energy μH of the magnetic moments μ remains negligible compared to the ortho−para fundamental energy ($\mu H \leq 1\ \text{cm}^{-1} \ll h\omega_{op} \approx 120\ \text{cm}^{-1}$). It is also negligible when compared to thermal energies ($\mu H \ll kT$) at the M.S. experimental temperatures ($150\ \text{K} < T < 350\ \text{K}$) and thus cannot affect the nuclear populations. Third, the conversion rate being a linear combination of o−p line intensities and each line intensity being invariant by any unitary transform of the wave functions, the conversion rate remains independent of the basis set. In particular, and provided that the magnetic energies remain much smaller than the rotational ones, the conversion rate can be estimated from zero-field wave functions. It is the purpose of this paper to suggest a resonant mechanism that leads to field accelerations of the conversion process. The general idea is that the transition energy can be drastically reduced when one nuclear o−p transition is counterbalanced by an opposite transition within the ionic electron system. In that case, the magnetic field becomes operative in modulating the transition energy.

In the (M.S.) experiments the hydrogen molecules, after being prepared in nonequilibrium o−p proportions, flow through the catalytic powder. Each molecule experiences many collisions on the grains surfaces. When a molecule hits a surface and is adsorbed, its motion parallel to the surface is more or less mobile until a collision from another molecule, or a phonon, produces the desorption. During its surface traveling, the molecule "visits" the 3d impurities where the o−p conversion occurs. The magnetic scatterings can be considered as independent events. The scattering times (about 10^{-11}−10^{-12}s) being much shorter than the conversion time ($\sim 10^{-3}$s), the resulting variation of ortho population during one collision remains infinitesimal ($\delta o \approx 10^{-8}$). One of the peculiarities of the M.S. experiments was the choice of hydrogen flow and catalyst mass that produced less than a moderate fraction of equilibrium populations. We shall therefore approximate the exponential return, toward the thermal equilibrium, to its initial slope (linear regime). If each molecule visits on the average N magnetic sites during its travel through the powder in a time T, the total variation of ortho population per unit of time equals $N\,\delta o/T$ as long as $N\,\delta o \ll 1$. Moreover, since the kinetic flow of molecular hydrogen (and thus N and T) cannot be modified by the application of small magnetic fields, we shall concentrate on the microscopic conversion δo during one scattering of average duration δt. The corresponding rate, $k = \delta o/\delta t$, can be obtained from the principle of detailed balance that we write in a formal way:

10.1021/jp990040t CCC: $18.00
Published on Web 05/27/1999

$$k = \sum_{i,j} P(o_i,p_j) W(o_i,p_j) J(\omega_{i,j}) \quad (1)$$

$P(o_i,p_j)$ represents a function of the initial and equilibrium populations of the ortho states o_i and para states p_j, and $W(o_i,p_j)$ represents the absolute square of the matrix element coupling these states. (It will not be necessary to specify the nature of the hyperfine interaction at work. Our subsequent analysis remains valid for any kind of o−p coupling.) $J(\omega_{ij})$ is the spectral density defined by the Fourier transform of the correlation functions, relative to the molecular motion and the phonons. It represents the ability of the energy transfer between the thermodynamic reservoir (thermal bath) and the quantum system composed of the impurity (and molecule) electrons and the hydrogen nuclei.[9−11] The indices i (respectively, j) denote all the electron and nuclear quantum numbers necessary to specify an ortho (respectively, para) eigenstate of the composed system. $h\omega_{ij}$ represents the energy separation between the electron−nuclear o_i and p_j eigenstates. In the following we shall use a Lorentzian form (exponential correlation functions) to model the spectral density:

$$J(\omega) = \frac{2\nu}{\omega^2 + \nu^2} \quad (2)$$

Its width ν is often described by an Arrhenius law: $\nu = \nu_0\, e^{-\beta\Delta E}$ where ν_0 is a prefactor (usually chosen as the frequency of the molecular vibration perpendicular to the surface, $\nu_0 \approx 10^{13}\ s^{-1}$). ΔE is an energy barrier that the molecule must overcome in order to escape from an adsorption site ($\Delta E \approx 1$ kcal/mol).

II. Electron−Nucleus Resonances

The rotational energies of a free hydrogen molecule are those of a free rotor: $BJ(J+1)$. Because the molecule is light, the rotational constant is large ($B \cong 60\ cm^{-1}$) and the ortho−para energy separations fall in the far-infrared. When the hydrogen molecule is physisorbed, it experiences the electric potential of the oxide catalyst that hinders the molecular rotation and splits the rotational levels, as represented in Figure 1a and 1b. The corresponding nuclear Hamiltonian, assumed to be of axial symmetry around the surface normal, has the following form:

$$H_n = B\mathbf{J}^2 + C_J(\mathbf{J}^2 - 3J_z^2) \quad (3)$$

Its eigenstates will be denoted (J, m). Depending on the potential shape (sign of C_J), a rotation parallel or perpendicular to the surface might be favored. In any case, numerical estimations and chromatographic measurement show that the induced splittings are about 150 cm^{-1}.[12−15]

To observe resonant effects between the nuclear and electron states, it is necessary that their energy levels be similarly split. Electronic splittings of a few hundreds of cm^{-1} can be induced by spin−orbit interactions when the electron orbital momentum is not quenched. We shall therefore assume that the many-electron ground state of the surface ions is degenerate. This implies, in turn, that one among the one-electron orbital states building this ground state is degenerate and only partially filled. This degeneracy can be related to the surface symmetry. A simple example of a 2-fold degeneracy might be found in the C_{4v} point group where the two 3d orbitals, pointing in two planes perpendicular to the surface, span the irreducible representation E. A similar 2-fold degeneracy also occurs in the C_{3v} symmetry (two different combinations of three 3d orbitals pointing in three perpendicular planes span the E representation of C_{3v}) and in different point group symmetries. In these cases, the n-electron orbital ground state is degenerate if this E state is only occupied by one electron. Introducing the electron spin, the spin−orbit interaction splits the ground state at first order. Let us first consider the simplified fine structure electronic Hamiltonian:

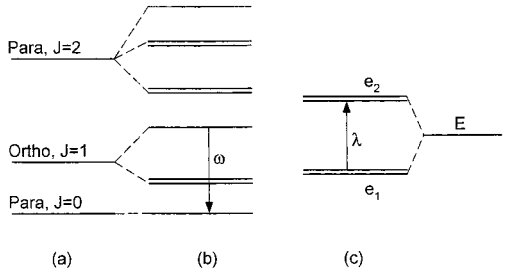

Figure 1. Nuclear and electron schematic energy levels: (a) first ($J \le 2$) rotational levels of an H_2 molecule and (b) their splittings by the catalyst surface potential; (c) spin−orbit splitting of one-electron 3d in an E state (the levels denoted e_1 (respectively, e_2) correspond to $\mu = 0$ (respectively, $\mu = \pm 2$), where $\mu = L_z + 2S_z$. One ortho−para transition, $(1, 0) \rightarrow (0, 0)$ is shown to be partially compensated by the electronic transition $e_1 \rightarrow e_2$ when $\lambda \approx \omega$.

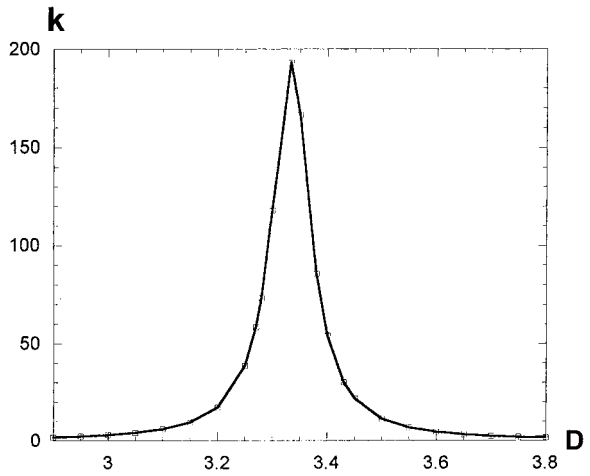

Figure 2. o−p conversion rate k (in s^{-1}) as a function of the rotation barrier strength D. ($\lambda = 300\ cm^{-1}$, $\nu = 1\ cm^{-1}$, $T = 150$ K).

$$H_e = \lambda \mathbf{L}\cdot\mathbf{S} - \mu_B \mathbf{H}\cdot(\mathbf{L} + 2\mathbf{S}) \quad (4)$$

L and **S** are the electron orbital and spin momenta of the impurity ion. λ denotes the strength of the spin−orbit interaction, which for 3d ions lies between and 200 and 300 cm^{-1}.[16−18] In the absence of a magnetic field it represents also the energy separation between two neighboring sublevels. In Figure 1c we have represented such a splitting in the simplest case of one-electron 3d ($n = 1$). The levels denoted e_1 (respectively, e_2) correspond to $\mu = 0$ (respectively, $\mu = \pm 2$), where $\mu = L_z + 2S_z$ and L_z (respectively, S_z) are the projections of **L** (respectively, **S**) on the surface normal. When the electron splitting λ equals one of the nuclear o−p energy separations ω, a resonance occurs in the conversion process. In that case one of the o−p transitions is exactly compensated by an opposite transition between two electron states of the catalyst ion, and the thermal bath has no energy to supply (or to absorb) this global transition. Consequently, the conversion rate is resonantly enhanced by 1 or 2 orders of magnitude. (Of course, the much stronger electron−phonon interactions maintain permanently the thermodynamical equilibrium within the electron system, and the thermal bath will still supply (or absorb) the o−p energy.) We have represented, in Figure 2, the o−p transition rate k as a function of the strength D of the rotation barrier. (D is here

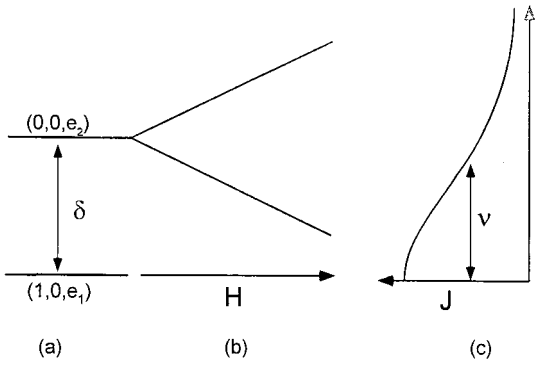

Figure 3. (a) Two nuclear−electron energy levels corresponding to the initial and final states of the transition indicated in Figure 1. (b) The ($J = m = 0$, e_2) level is split by an applied magnetic field, whereas the ($J = 1$, $m = 0$, e_1) one is not ($\mu = 0$). (c) The spectral density J of width ν is represented centered on the para state as a function of transition energy.

defined by $C_J = BD[(2J - 1)(2J + 3)]^{-1}$). This spectrum presents a resonance relative to the transition between the ortho levels ($J = 1$, $m = \pm 1$) and the para ($J = 2$, $m = \pm 1$) ones around $D = 3.33$. The corresponding resonant enhancement exceeds 2 orders of magnitude. The conversion rate was estimated by assuming a dipole−dipole magnetic interaction between the electron and nuclear spins, as described in ref 19, but since the resonance appears in the spectral density, it remains independent of the particular angular coupling.

Quite generally, the resonance condition $\lambda = \omega$ is not exactly fulfilled, and we shall denote by $\delta = \lambda - \omega$ the energetical deviation from it. Then, the application of a magnetic field H will bring a subset of levels closer to the resonance. In Figure 3 we have represented two particular electron−nucleus energy levels, one of which being split by H. When the width ν of the spectral density J is of the order of the magnetic Zeeman energy (~ 1 cm^{-1}) and smaller than the initial energy separation δ, the closer approach of one sublevel enhances more the conversion rate than the decrease produced by the remoteness of the other sublevel.

III. Magnetic Field Accelerations

The magnetic field acceleration is defined by the relative variation of the conversion rate:

$$\gamma(H) = \frac{\langle k(H) - k(0)\rangle}{\langle k(0)\rangle} \tag{5}$$

where $k(H)$ represents the conversion rate in the presence of a magnetic field H. The rate averages must be introduced because the experiments were performed on powders. The surfaces of the grains being rather irregular, the surface potentials above each magnetic site are not necessarily exactly identical. Consequently, the separations δ vary from site to site. Moreover, the orientation of the surface normal with respect to the applied magnetic field differs at each site. (It is, however, simpler to fix the surface normal and average over all the relative orientations of the magnetic field.) The important point to stress is that when the electron−nucleus system presents a resonance, all the remaining o−p transitions become negligible compared to the one satisfying even approximately the resonance condition. In other words, the crossing of two electron−nucleus energy levels singles out that particular transition. Consequently, the magnetic field acceleration reduces to the relative variation of the spectral density induced by the application of the magnetic field:

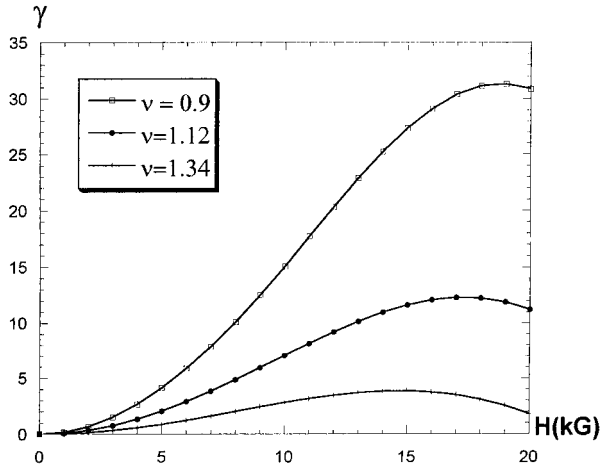

Figure 4. Magnetic field acceleration γ vs the applied magnetic field H (in kG) for three values of the spectral width ν ($T = 150$ K, $\delta = 1$ cm^{-1}).

$$\gamma(H) \cong \frac{\langle J(\delta_H) - J(\delta)\rangle}{\langle J(\delta)\rangle} \tag{6}$$

where $J(\delta_H) = (1/p)\sum_p J(\delta_p)$ and $J(\delta_p)$ is the spectral densities at the frequencies δ_p corresponding to the transitions between the unsplit level and the p sublevels split by H (in the model of Figure 3, $p = 2$).

We have calculated the field accelerations for a variety of fine structures and surface potentials and by using Gaussian distributions of δ values (and uniform distributions for the field orientations) to represent the site averages. However, to clarify the field acceleration patterns, we shall first assume that the approximate resonance (small δ) is identically satisfied by all the catalyst surface sites. We have represented, in Figure 4, $\gamma(H)$ as a function of the applied magnetic field for different values of the spectral width ν and for $\delta = 1$ cm^{-1}. The initial growth of the field acceleration appears quadratic, then it is followed by a linear increase until it approaches a maximum. After the maximum, the involved levels move too far apart and consequently the acceleration decreases. The saturation observed in the M.S. experiments seems to correspond to this maximum. We shall return to this point after introducing a distribution of δ values. Figure 4 displays the sensitivity of the magnetic acceleration upon the relative values of δ and ν. In accordance with intuitive expectation the field acceleration is maximum for $\delta \approx \nu$, and more precisely, δ slightly larger than ν. For a sharp acceleration, the splitting level must lie outside, but close to, the efficient region (defined by the width ν of the spectral density). Let us also remark that ν should be of the order of 1 cm^{-1} in order that the magnetic field H shifts one of the split levels toward the resonance. Such a value can be obtained for an energy barrier ΔE (against the surface motion) larger than the thermal energy (for instance, at $T = 150$ K, $\Delta E \approx 1.5$ kcal/mol), which corresponds to a rather localized adsorption. In Figure 5, we represent the field acceleration as a function of δ for fixed values of the applied magnetic field ($H = 20$ kG) and the spectral width ν ($\nu = 0.42$ cm^{-1}). For $\delta = 0$ (exact resonance), γ is negative, since the magnetic sublevels split symmetrically with respect to the unsplit ones. However, on each side of the resonance, γ becomes positive, reaches a high maximum (300% for the chosen set of parameters), and decreases as the system moves away from the resonance. We remark that, within the depicted model, the field acceleration remains observable up to about 5 cm^{-1} on each side of the resonance.

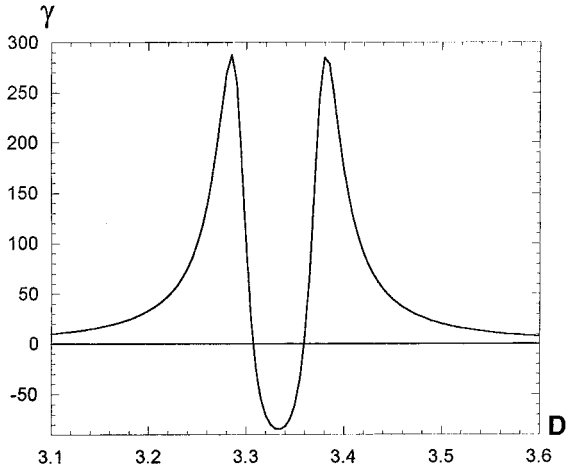

Figure 5. Magnetic field acceleration as a function of the rotation barrier strength D ($T = 150$ K, $H = 20$ kG, $\nu = 0.42$ cm^{-1}). The resonance occurs at $D = 3.33$ ($\delta = 0$), and, around, δ and D are related by $\delta = 80 - 24D$ (in cm^{-1}).

The position of the resonances being directly related to the surface electric potential, simple pretreatments of the catalyst surface are able to improve the catalyst yield. For instance, in the M.S. experiments,[6] a 0.0028% sample of chromia dispersed on alumina after 2.5 h of pretreatment in H_2 at 490 °C gave an acceleration of 25% in a magnetic field of 7.5 kG at −150 °C. The identical sample after 2 h of pretreatment in H_2 at 535 °C gave an acceleration of 75% and a moderately smaller zero field conversion under identical experimental conditions. By considering the graphs of the conversion rate and the field acceleration as functions of the surface electric potential, represented in the Figures 2 and 5, it may be concluded that the second pretreatment has slightly shifted the system away from the resonance. This example displays the sensitivity of the magnetic field acceleration upon catalyst pretreatments and its practical usefulness in the selection and preparation of o−p catalysts.

Up to now our model of the electron−nucleus system is rather simplified. For a more realistic one it is necessary to introduce the interactions of the rotational molecular momentum with the spin and angular momenta of the electrons. These interactions lead to more complex fine structures, and more electron−nucleus levels can be brought simultaneously in near-coincidence. In the following we shall consider the following electron−nucleus Hamiltonian:

$$H = H_e + H_n + H_{e-n} \tag{7}$$

$$H_{e-n} = t\mathbf{J}\cdot\mathbf{S} + \theta\mathbf{J}\cdot\mathbf{L} \tag{8}$$

In Figure 6, we represent the crossings of the electron−nucleus levels corresponding to the para states ($j = 2$, $m = 1$) and ortho ones ($j = 1$, $m = 1$) relative to the two electon states e_1 and e_2. We have represented, in Figure 7, the field acceleration relative to the transitions depicted in Figure 6, as a function of δ and for a fixed value of the applied magnetic field ($H = 20$ kG). We obtain twice the number of curves represented in Figure 5, since Figure 6 contains twice as many transitions as in Figure 3. Figure 7 presents also two resonances at $\delta = \pm 2$ cm^{-1}. Therefore, the corresponding field acceleration extends over a wider range (about 10 cm^{-1} around $\delta = 0$). An example of such field accelerations as functions of the applied magnetic field and for different values of δ is given in Figure 8. The initial acceleration (at low field) appears steeper and the

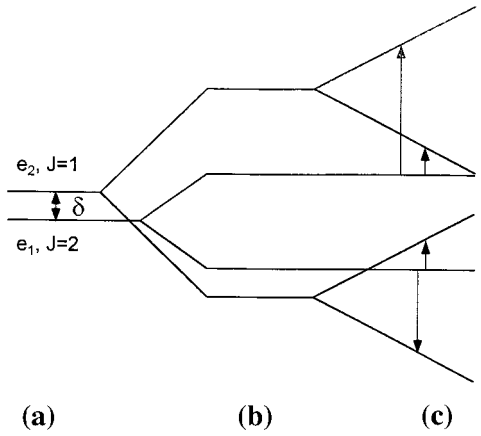

Figure 6. Two nuclear−electron energy levels in the vicinity of a resonance. (a) The para (ortho) level $J = 2$ ($J = 1$) is associated with the electron state e_1 (e_2). (b) These levels are split by the interactions between the electron and nuclear angular momenta. (c) The set (e_2, $J = 1$) is further split by an applied magnetic field H.

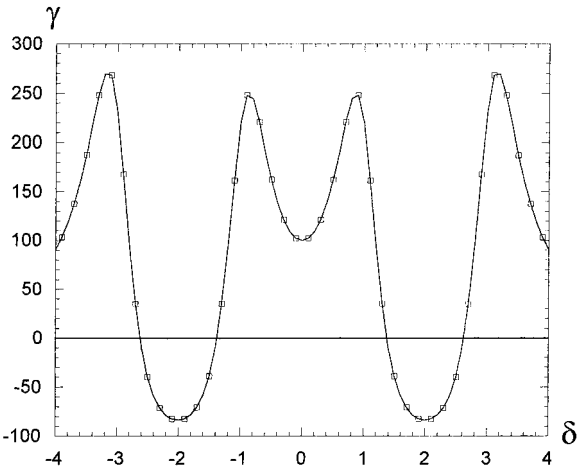

Figure 7. Magnetic field acceleration as a function of the energy deviation δ (in cm^{-1}). ($T = 150$ K, $H = 20$ kG, $\nu = 0.42$ cm^{-1}, $\theta = 1$ cm^{-1}, $t = 2$ cm^{-1}).

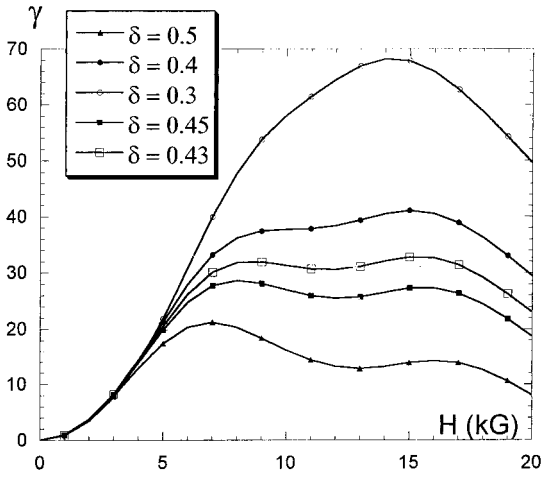

Figure 8. Conversion acceleration vs the applied magnetic field H (in kG) at $T = 150$ K and for different values of the energy deviation δ (in cm^{-1}) ($\theta = -0.5$ cm^{-1}, $t = 1$ cm^{-1}, $\nu = 0.42$ cm^{-1}).

"plateau" around the maximum much wider. Now by choosing a Gaussian distribution of δ values (centered around 0.4 cm^{-1} with a standard deviation of 0.03 cm^{-1}) representing some average over the sites of the powder, we obtain the field acceleration, represented in Figure 9. This curve is compared

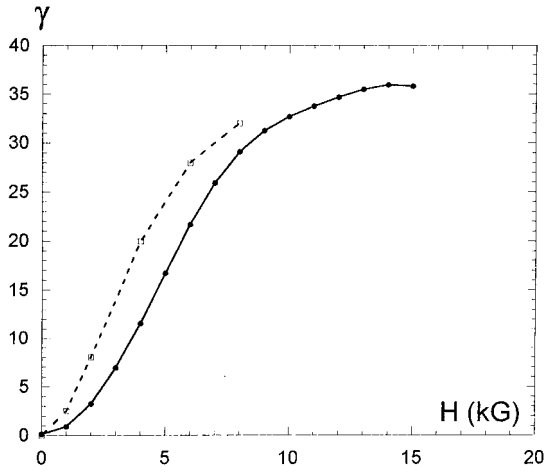

Figure 9. Conversion acceleration vs the applied magnetic field H (in kG) at $T = 300$ K. The dashed curve represents the experimental acceleration over a sample of 0.17% Cr_2O_3 supported on α-Al_2O_3 (from ref 6). The full curve represents the theoretical one calculated with $\lambda = 200$ cm^{-1}, $\nu = 0.42$ cm^{-1}, and a Gaussian distribution of δ values centered around 0.4 cm^{-1}, with a standard deviation of 0.03 cm^{-1}.

to a measured field acceleration observed by Misono and Selwood, and the concordance appears quite satisfactory. Both curves are composed of a quadratic initial increase at very low fields ($H < 2$ kG), followed by a linear increase at intermediate fields (2 kG $< H <$ 6 kG), and saturated at high fields ($H > 10$ kG). The quadratic initial increase seems more pronounced in the theoretical curve than in the experimental one, but it is difficult to draw any definite information about this slight difference. First, at low field, we have only one experimental point at our disposal, and the line joining the first two points does not intersect the origin. Second, we must keep in mind that our model includes a few simplifying assumptions and thus remains essentially qualitative. Particularly at low field, where the precise form of the spectral density becomes crucial, our Lorentzian model is rather crude. More precise ones, such as those detailed in ref 10, should be introduced. As concerns the saturation part, the simple maximum obtained for a single value of δ has been replaced by a large "plateau" and the subsequent acceleration decrease shifted toward much higher values of the magnetic field. The width of the "plateau" is directly related to the distribution width of δ, and it is the superposition of the different maxima, included in the average over the δ values, that has led to the observed saturation. This saturation is apparent, and the validity of our model could be checked by performing experiments at higher fields to observe the subsequent acceleration decrease.

IV. Concluding Comments

The modification of a chemical reaction by a magnetic field and/or a magnetic catalyst has long been the subject of controversial debates.[20,21] Many different interpretations have been proposed, and we do not know presently whether the herewith described resonant mechanism might be extended and applied to different chemical reactions.

Let us summarize the necessary conditions that must be satisfied by the electron−nucleus system to observe a magnetic field acceleration of the o−p hydrogen conversion rate on transition oxides of the iron series.

(i) The electron orbital ground state of the catalyst transition ion must be degenerate in order that the spin−orbit interaction removes this degeneracy at first order.

(ii) One of the o−p transition energies must be approximately equal to the electron spin−orbit splitting. We recall that the o−p energies strongly depend on the electric potential created by the oxide charges.

(iii) The width of the thermal spectral density of the adsorbed molecules must be of the order of the magnetic Zeeman energy (∼1 cm^{-1}).

(iv) A minimum and negative magnetic field acceleration is obtained when the electron−nucleus system is at an exact resonance.

(v) When the energetical deviation from resonance is of the order of the width of the spectral density, a positive magnetic field acceleration is observed. When it slightly exceeds the width, the field acceleration reaches a maximum.

Note that the distinction between cases iv and v might be obscured by the surface potential averages and by superposed near resonances. Consequently, the resulting magnetic field acceleration can be successively negative and positive, as observed on a CoO catalyst.

If a magnetic field acceleration is observed experimentally in the o−p hydrogen conversion on a transition oxide, it is possible to conclude that the catalyst is operating near a crossing of electron−nucleus energy levels. At exact resonance, the conversion rate displays a peak, the magnetic acceleration is negative, and the catalyst is working at maximum efficiency. Since the positions of the resonances are directly related to the surface electric potential, simple pretreatments of the catalyst surface are able to improve the catalyst yield. The magnetic field effects could be used to determine how efficiently a catalyst is operating and to control its improvement. The sensitivity of the magnetic field acceleration upon catalyst pretreatments may thus have important practical applications in the selection and preparation of industrial catalysts.

References and Notes

(1) Farkas, A. *Orthohydrogen, Parahydrogen and Heavy Hydrogen*; Cambridge University Press: London, 1935.
(2) Wigner, E. *Z. Phys. Chem B.* **1933**, *23*, 28.
(3) Schmauch, G. E.; Singleton, A. H. *Ind. Eng. Chem.* **1964**, *56*, 20.
(4) Wakao, N.; Smith, J. M.; Selwood, P.W. *J. Catal.* **1962**, *1*, 62.
(5) Misono, M.; Selwood, P. W. *J. Am. Chem. Soc.* **1968**, *90*, 2977.
(6) Misono, M.; Selwood, P. W. *J. Am. Chem. Soc.* **1969**, *91*, 1300.
(7) Ng, C. F.; Selwood, P. W. *J. Catal.* **1976**, *43*, 252.
(8) Selwood, P. W. *Adv. Catal.* **1978**, *27*, 23.
(9) Ilisca, E.; Legrand, A. P. *Phys. Rev. B.* **1972**, *5*, 4994.
(10) Petzinger, K. G.; Scalapino, D. J. *Phys. Rev. B* **1973**, *8*, 266.
(11) Ilisca, E. *Prog. Surf. Sci.* **1992**, *41*, 217.
(12) McRury, T. B.; Sams, J. R. *Mol. Phys.* **1970**, *19* (3), 337.
(13) Moore, W. R.; Ward, H. R. *J. Am. Chem. Soc.* **1958**, *80*, 2909.
(14) Mortensen, E. M.; Eyring, H. *J. Phys. Chem.* **1960**, *64*, 433.
(15) King, J.; Benson, S. *J. Chem. Phys.* **1966**, *44*, 1007.
(16) Abragam, A.; Bleaney, B. *Electron Paramagnetic Resonance of Transition Ions*; Clarendon Press: Oxford, 1970.
(17) Blume, M.; Watson, R. E. *Proc. R. Soc. A* **1963**, *271*, 565.
(18) Francisco, E.; Pueyo, L. *Phys. Rev. B* **1988**, *37*, 5278.
(19) Makoshi, K.; Rami, M.; Ilisca, E. *J. Phys.: Condens. Matter* **1993**, *5*, 7325.
(20) Figueras Roca, F. *Ann. Chim.* **1967**, *2*, 255.
(21) Atkins, P. W.; Lambert, T. P. *Ann. Rep. Chem. Soc. A* **1975**, *72*, 67.